LIMNOLOGY
and
OCEANOGRAPHY: METHODS

ASLO

Limnol. Oceanogr.: Methods 24, 2026, e70011
© 2025 The Author(s). *Limnology and Oceanography: Methods* published by Wiley Periodicals LLC on behalf of Association for the Sciences of Limnology and Oceanography.
doi: 10.1002/lom3.70011

NEW METHODS

pamfit: A new R package for spatially resolved analysis of Imaging PAM photosynthesis–irradiance light curve parameters

B. Jesus,[1] P. Cartaxana,[2] C. Williamson [3]*

[1]Nantes Université, Institut des Substances et Organismes de la Mer, Nantes, France; [2]Laboratory for Innovation and Sustainability of Marine Biological Resources (ECOMARE), Centre for Environmental and Marine Studies (CESAM), Department of Biology, University of Aveiro, Aveiro, Portugal; [3]Bristol Glaciology Centre, School of Geographical Sciences, University of Bristol, Bristol, UK

Abstract

Imaging Pulse Amplitude Modulation (PAM) fluorometry allows spatially resolved measurements of Photosystem II (PSII) fluorescence kinetics through time without disturbing study organisms or their environments. In particular, the use of photosynthesis–irradiance curves (P–I curves) provides detailed information on PSII quantum efficiency, electron transport rates and the overall photosynthetic performance of samples. Here, we present the R "*pamfit*" package developed as a Shiny application to significantly extend current analysis capabilities for Imaging PAM P–I curve datasets. Through a sequential Shiny user interface, *pamfit* allows to (i) import Imaging PAM TIFF P–I curve datasets, assign light levels and employ pixel smoothing; (ii) define a region of interest for subsequent modeling; (iii) derive optimal start parameters and fit one of three P–I curve models—Jassby and Platt, Platt et al., or Eilers and Peeters; and (iv) undertake pixel-wise interrogation of both initial data and derived P–I curve parameters including, light utilization (α) and saturation (E_k) coefficients, maximum electron transport rates (ETR_{max}), photo-inhibition coefficients (e.g., β when derived), and associated residual mean square error (RMSE) images. Outputs can be saved in GeoTIFF or CSV format and exported to the R global environment for subsequent processing. We present here example applications of *pamfit* to three P–I curve datasets for the photosynthetic sea slug *Elysia timida*, a microphytobenthic biofilm, and the coralline seaweed *Corallina officinalis*, chosen because they exhibit high spatial variability. The flexibility of processing images using free open-source software extends the usefulness of this technique and holds great potential for application in ecophysiological studies.

Imaging Pulse Amplitude Modulation (PAM) fluorometry allows simultaneous capturing of both spatial and temporal variability in Photosystem II [PSII] quantum efficiency for a large range of phototrophic organisms and is now routinely employed as a powerful tool in many ecophysiological studies (Omasa et al. 1987; Vieira et al. 2013; Leal et al. 2014; Perkins et al. 2016; Jesus et al. 2022). The ability to quantify spatial variability in PSII kinetics is particularly important when attempting to estimate the primary productivity of highly heterogenous phototrophic surfaces, for example, microphytobenthic biofilms, which are difficult to characterize without high sampling replication (e.g., Guarini et al. 2002; Jesus et al. 2005). Assessing spatial variability is equally important when studying the distribution and regulation of photosynthetic potential across sub-cellular (e.g., chloroplasts) and whole tissue (e.g., fronds/leaves) scales (Perkins et al. 2016; Jesus et al. 2022).

A commonly employed Imaging PAM-based tool available to probe photosynthetic potential is the application of photosynthesis irradiance curves (P–I curves) techniques, whereby samples are typically exposed to increasing steps of irradiance from light-limiting to light-saturating conditions, with corresponding pixel-wise imaging of PSII fluorescence kinetics

*Correspondence: c.williamson@bristol.ac.uk

This is an open access article under the terms of the Creative Commons Attribution License, which permits use, distribution and reproduction in any medium, provided the original work is properly cited.

Associate editor: Tammi Richardson

during saturating pulse measurements (Ralph et al. 2005; Nielsen and Nielsen 2008; Lichtenberg et al. 2017; Serôdio et al. 2013; Jesus et al. 2023; Morelle et al. 2024). From these, electron transport rates through PSII can be calculated and modeled against irradiance to estimate parameters commonly used in modeling primary productivity, for example, light utilization and light saturation coefficients, maximum electron transport rate and coefficient of photo-inhibition; α, E_k, ETR_{max} and β, respectively (Nielsen and Nielsen 2008; Lichtenberg et al. 2017; Serôdio et al. 2013; Jesus et al. 2023; Morelle et al. 2024).

Current Imaging PAM proprietary software does not calculate derived P–I curve parameters directly. Instead, the electron transport rate for a given light level can be calculated and plotted for specific regions of interest (ROI), which are summarized as mean values. This procedure not only removes any potential spatial variability inside the ROI but also prevents contiguous analysis of photosynthetic potential across the complete photosynthetic surface. To fully explore the spatial variability in sample photophysiology, it is preferable to create and utilize complete images of the P–I curve derived parameters, avoiding ROI averaging. This requires that each image pixel is treated as a separate ETR value and that models are fitted in a pixel-wise manner corresponding to the separate light curve levels. Although Imaging PAM fluorescence has been available for over 25 years, this has remained beyond the current capabilities of proprietary software.

In the current work, we present *pamfit*: an R package (R Core Team 2025) with a Shiny interface (Cheng et al. 2024) to analyze TIFF images exported from the Imaging PAM fluorometer to produce P–I curve parameter images (e.g., α, E_k, ETR_{max}, and β), for all image pixels. Here we apply this method to three photosynthetic surfaces to demonstrate the potential of exploring P–I curve parameter images without previous ROI selection. Photosynthetic sea slugs (*Elysia timida*), microphytobenthic biofilms and *Corallina officinalis* alga were chosen as examples because they are known to exhibit high spatial variability (e.g., Gerbersdorf et al. 2005; Perkins et al. 2016).

Materials and procedures

The *pamfit* package

The *pamfit* R package is available for download and installation from https://github.com/bmjesus/pamfit, where a complete user guide can also be found with example datasets. The general procedure is: (1) export P–I curve data from the imaging PAM proprietary software in TIFF (.tif) format (i.e., Imaging Win, Walz GmbH); (2) launch the Shiny app in R with the command *pamfit()*; (3) upload the TIFF file, input light levels either directly or by upload of a text file (.txt), smooth images if desired, and select ETR calculation in either relative units (default) or using absorptivity imagery if available; (4) select an ROI for subsequent modeling, which can be the entire image; (5) use example pixels to determine optimal starting parameters and fit the preferred model to each pixel of the P–I curve dataset; and finally, (6) view, analyze and export the initial and derived P–I curve parameter images at a pixel-by-pixel resolution. We provide a brief outline of the *pamfit* workflow below, though we advise consulting the complete user guide before utilizing the package.

To install *pamfit* from GitHub, the user first needs to install the package *devtools* (Wickham et al. 2022). Once *devtools* is installed and loaded the user can use the function *install_github()* to install *pamfit* directly, that is, *install_github* ("*bmjesus/pamfit*"). This function will also install all *pamfit* dependencies. *pamfit* uses functions from 20 other packages. Thus, depending on your current R setup this step might take some time.

Shiny app workflow

Imaging PAM P–I curves export

Saving an Imaging PAM P–I curve in TIFF (.tif) format using the ImagingWin software (Walz, ImagingWin v2.33) produces a multi-layered TIFF file that includes the following images in their respective order: F_o, F_m, Near Infra-Red (NIR), Red, followed by sequential F_o/F_m or F'/F_m' images for each light step of the P–I curve (*see* Supporting Information Table S1 for fluorescence nomenclature). As the initial two images of the TIFF file (F_o, F_m) can be held over from a previous sample dependent on ImagingWin settings, *pamfit* utilizes the subsequent F_o/F_m images consistently located in positions five and six of the TIFF file, representing the first dark measurements of the P–I curve. While NIR and Red images are not always collected by users undertaking P–I curves with an Imaging PAM fluorometer, ImagingWin software inputs black images in these positions regardless. Thus, the number of images within the P–I curve TIFF file allows *pamfit* to identify the number of light steps of the P–I curve for subsequent processing.

Upload image

Loading the *pamfit* R package adds a function called *pamfit()* to the R environment, which launches a Shiny app interface. The user is prompted to upload their P–I curve TIFF file, which results in the rendering of a light level input table and an F_o image plotted within an interactive interface. Users can either input light levels per light step into the rendered table or upload a .txt file containing this information. Light levels are saved in a hidden R environment to prevent the requirement to upload light levels repeatedly when processing data from the same P–I curve setup within the same R session. Two optional steps include the smoothing of pixels to remove noise from the original images, whereby the user selects the number of pixels to average; and a second step to choose if absorptivity data should be used in electron transport rate calculations (ETR). To end the first stage, the user needs to confirm their choices. After confirmation, the app calculates ETR values for each pixel and each light step, producing an ETR

image per light step. If no absorptivity data is available, ETR images are calculated as: $ETR = 0.5 \times F_q'/F_m' \times PAR$, where $F_q' = (F_m' - F')/F_m'$ (Oxborough et al. 2000). When absorptivity data ($Abs = 1 - Red/NIR$) are available and selected to be used in ETR calculations, images are calculated as: $ETR = 0.5 \times F_q'/F_m' \times PAR \times Abs$.

Select ROI

The second stage consists of defining a region of interest (ROI) for processing. The user can define irregular polygons, rectangles or circles, with any pixel outside of the ROI reclassed as non-value (NaN). The ROI can be any size required, including the entire image if desired. Options are available to export the ROI coordinates to be used again if wanted, and to import previously defined ROI as a text file (.txt). Subsequent processing time will increase with the number of pixels to process, but this can be reduced if parallel processing is available.

Select fit parameters

After ROI selection, *pamfit* asks the user to select which model to fit to the P–I curve ETR data and to select how many light steps to use in modeling. The user can select a subset of the available light levels to fit the model to. This is particularly useful in the case the user wants to remove some of the last light levels. Currently, *pamfit* is designed to process standard incremental light curves, such that for protocols with a recovery measurement at the end of the light curve, the user will need to omit the final measurement point here prior to processing. To test the effect of fitting different models and/or numbers of light steps, an interactive image is rendered for the user, who can click any pixel to view the associated P–I curve ($ETR \sim PAR$) plot, select one of three models to fit (*see* below) and overlay on the plot, with a dropdown menu available to clip the P–I curve to any number of light steps > 4. Importantly, the associated P–I curve derived parameters that are shown for the selected pixel are used as starting values in subsequent modeling of all pixels of the ROI—thus the user should ensure to select a pixel in a zone representative of the image to maximize model convergence for as many pixels as possible. If the user wishes to analyze a new ROI, they must either refresh pamfit using the global refresh option or click the "Reset" button in this step to remove previous light subsets and model parameters.

pamfit allows fitting one of three P–I curve models to Imaging PAM datasets: the Jassby and Platt (1976) model that does not include a photoinhibition component, shortened in the remaining text to Jassby model; the Platt et al. (1980) model that includes a photoinhibition parameter (β), shortened in the remaining text to Platt model; and the Eilers and Peeters (1988) model that also includes a component to take into account photoinhibition (E_{opt}), shortened in the remaining text to EP model. All models are fitted with the "nlsLM" function of the minpack.lm R package (Elzhov et al. 2023) using the PORT non-linear least-squares algorithm. This function also returns uncertainty values, provided in *pamfit* as images of the standard error for all estimated parameters and the residual mean squared error (RMSE) for the global fit. Given that pixel-wise fits can be computationally expensive for large ROI, *pamfit* provides the option to increase the number of Central Processing Unit (CPU) cores to use in full ROI processing from the default of 1. The number of CPU cores available is automatically detected and the optimal number used depends on the hardware available and the size of the image. Once all settings are decided, the user confirms and the model is fitted pixel-wise to the entire ROI.

View and export data

Model fitting produces images of the derived parameters of the respective P–I curve model chosen, as well as images of associated errors of fit. *pamfit* then allows viewing, analyzing, and exporting these results as well as the initial raw datasets uploaded to the app. Any parameter can be selected for interactive plotting and the user can further apply graphical tools (transects or polygons) to select regions/transects of interest for closer inspection. Once an area or transect is defined, a new tab will appear, showing plots of the individual pixel values. The user can plot any combination of two parameters for their selected pixels as well as examine the distribution of any parameter along the transect.

The entire complete dataset including derived P–I curve parameters or any individual parameter for the entire modeled region can be: (i) saved as a GeoTIFF file; (ii) saved as a comma-separated value file (.csv) file; or (iii) exported to the R global environment as a user-defined named list of objects. Likewise, ROI or transect data delineated using the visualization tools within *pamfit* can be saved as a text file (.csv) file, whereby every available parameter for the selected pixels is saved, or exported as a dataframe object to the R global environment. Datasets exported to the global environment are available for subsequent visualization and analysis once the *pamfit* app is closed. Multiple ROI/transect datasets can be produced and exported to R as desired but they will only be visible once *pamfit* is closed. The settings tab allows viewing and saving (as .csv) all settings applied throughout the *pamfit* workflow.

Load pre-processed GeoTiff

Functionality is included in *pamfit* to re-load *pamfit* outputs for further modeling, visualization and analysis. In this case, *pamfit* only accepts GeoTiff outputs of complete datasets previously exported as such following completion of the *pamfit* workflow. On upload, much of the *pamfit* functionality becomes re-available to the user for their dataset, including the option to apply a different P–I curve model to their dataset and/or model ETR for a different number of light steps. Importantly, though, these analyses are restricted to the original ROI defined on the original raw data uploaded to the app, and any smoothing applied to the original dataset is retained here.

Assessment

Below, we present three brief examples of applying *pamfit* to Imaging PAM fluorescence P–I curve datasets from samples exhibiting strong spatial variability in their photosynthetic properties: the photosynthetic sea slug *E. timida*, a diatom-dominated microphytobenthic biofilm, and the red coralline macroalga *C. officinalis*. However, we emphasize that *pamfit* is broadly applicable to any photosynthetic sample or surface analyzed using Imaging PAM fluorescence P–I curve techniques, particularly in cases where spatial heterogeneity is of interest (e.g., plant leaves, coral surfaces).

Biological material

Sacoglossan sea slugs (Opisthobranchia) can extract chloroplasts from the algae they consume, incorporate them into their cells, and maintain their photosynthetic function for extended periods (Costa et al. 2012; Cartaxana et al. 2019). These stolen chloroplasts, known as kleptoplasts, are retained within the cytosol of cells surrounding the digestive tract and can contribute to the slug's metabolism (Cartaxana et al. 2021). Since the digestive system of sea slugs is highly branched and distributed throughout the body, the spatial distribution of kleptoplasts varies considerably across the mollusk's surface. In this study, *E. timida* specimens were collected by snorkeling in the Mar Menor coastal lagoon, Mediterranean Sea (Jesus et al. 2010). Before imaging PAM fluorescence P–I curve analysis, the specimens were placed inside a concave microscopy slide to facilitate measurement in a leaf-like position without causing harm to the animals.

Microphytobenthic (MPB) biofilm sediment samples were collected from the Alcochete intertidal flat, Tagus Estuary, Portugal, during low tide in September 2012, using Plexiglas corers (8 cm internal diameter). The sampled sediment was predominantly muddy, with 97% of particles measuring less than 63 μm in diameter. Before conducting Imaging PAM P–I curve analysis, sediment was sub-sampled from the original cores using circular (20 mm diameter) Plexiglas minicores. The microphytobenthic community consisted exclusively of diatoms, primarily motile epipelic species from the genera *Navicula* and *Gyrosigma* (Vieira et al. 2013).

Specimens of the coralline red seaweed *C. officinalis* were collected in September 2015 from tidal pools at La Pointe St-Gildas on the French Atlantic coast. The example presented in this paper is part of a larger dataset previously reported by Perkins et al. (2016), in which an earlier version of the code, now integrated into the *pamfit* Shiny app, was applied. The sample used in this study was collected from the lower shore, where *C. officinalis* fronds were heavily colonized by diatom epiphytes, thereby maximizing spatial variability in the calculated P–I curve parameters.

PAM fluorescence methodology and data processing

All fluorescence measurements were conducted using Imaging PAM fluorometers (Walz, Effeltrich, Germany). *Corallina officinalis* was imaged with the Maxi version, while *E. timida* and the microphytobenthic biofilm were both imaged using the Mini version of the Imaging PAM M-Series (Walz, Effeltrich, Germany). Both Imaging PAM fluorescence systems were equipped with IMAGE-K5 1/2″ CCD cameras, producing images at a resolution of 640 × 480 pixels using a blue LED array. The LED array provided the measuring beam, actinic light, and saturating light pulses. Saturation pulse intensity was set to 6000 μmol photons $m^{-2}\,s^{-1}$, with a duration of 0.8 s and a measuring pulse frequency of 8 Hz. For P–I curves, samples were exposed to 10 to 14 increasing actinic light intensities, ranging from 0 to 1200 μmol photons $m^{-2}\,s^{-1}$ for *E. timida*, 0 to 996 μmol photons $m^{-2}\,s^{-1}$ for the microphytobenthic biofilm, and 0 to 531 μmol photons $m^{-2}\,s^{-1}$ for *C. officinalis*. Each irradiance step lasted 30 s. P–I curve image datasets were exported from the Walz ImagingWin software as TIFF files using standard settings and imported into *pamfit* for all subsequent data analysis. After generating the P–I curve parameter images, the results were exported to the R workspace for further analysis and to create the figures presented below.

Statistics and hardware

All tests and figures were generated on a Dell Precision 7680 laptop equipped with a 13th Gen Intel® Core™ i9-13950HX (32 threads), 64 GB of RAM, and running Ubuntu 22.04.5 LTS.

Comparisons between images or ROI pixel values were performed using Kruskal–Wallis tests, following assessments of normality with Shapiro–Wilk tests and homogeneity of variance with Levene's test. All statistical analyses were conducted in R version 4.4.3 (R Core Team 2025).

Image smoothing

Applying smoothing to the input images had a significant effect on all samples, primarily by reducing the global RMSE (Fig. 1). Most of the improvement occurred between applying no smoothing and the first smoothing level (i.e., 3 pixels), resulting in an RMSE decrease of 60%, 56%, and 35% for *E. timida*, MPB, and *Corallina*, respectively. Beyond 5 pixels, the reduction in RMSE was minimal, and detailed spatial structures began to blend into the background (Supporting Information Fig. S1).

The optimal level of smoothing likely depends on several factors, including the total number of pixels in the image, the instrument's gain (as higher gain increases electronic noise), and the sample type. In our case, the greatest improvements were observed for the sea slug, which was expected, as the animal moved slightly between light steps. Although the movement was minimal, it was sufficient to misalign some pixels between light steps. Averaging the surrounding 3 pixels helped reduce this noise (Fig. 1A). While increasing smoothing beyond 5 pixels continued to lower RMSE, the trade-off of losing finer spatial structures would likely be undesirable for users focused on the spatial heterogeneity of photosynthetic parameters. Therefore, we selected a smoothing level of 5 pixels for all analyses described in the following sections.

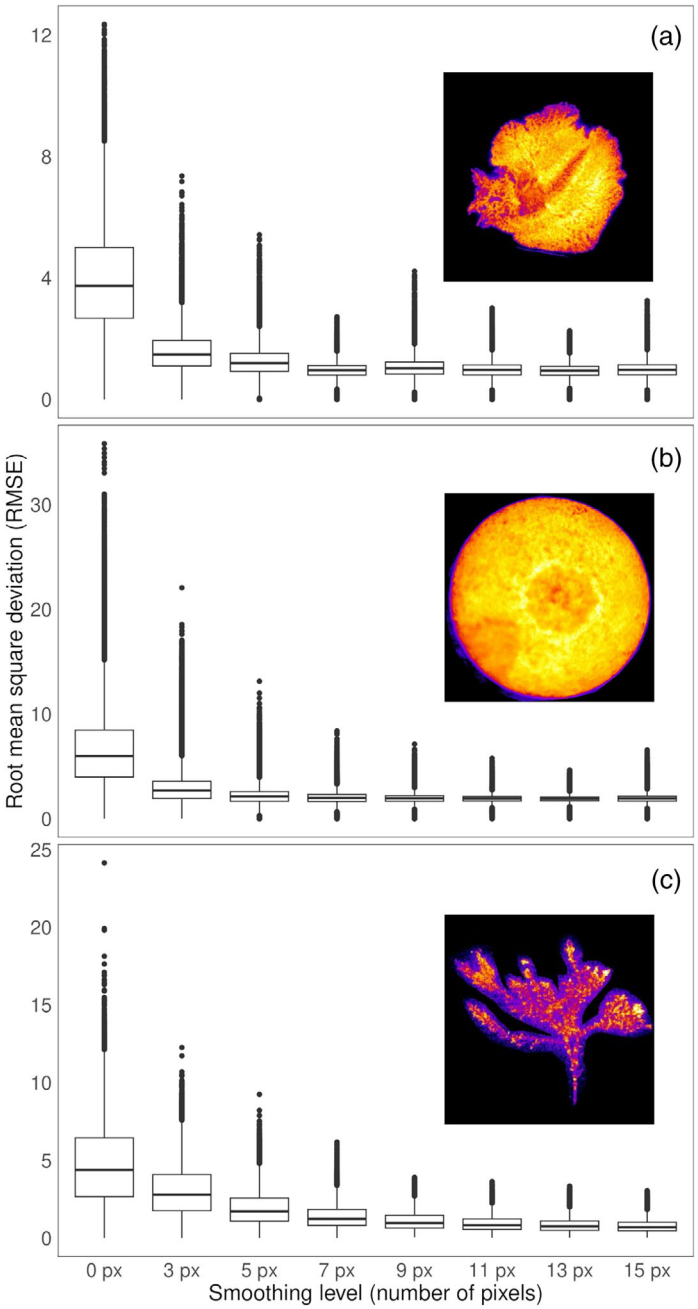

Fig. 1. Smoothing effect on root mean square error (RMSE). (**a**) *Elysia timida* sea slug; (**b**) Microphytobenthic biofilm; (**c**) *Corallina officinalis* macroalgae frond. Insets at each plot constructed using minimum fluorescence (F_o) images of each sample. Residual mean square error values calculated after fitting the Eilers and Peeters (1988) model and represented as boxplots for each smoothing level.

Model selection and fitting starting values

Selecting the appropriate model and accurate starting values is crucial for obtaining reliable results in non-linear fitting procedures. The non-linear iterative algorithm used to fit photosynthesis–irradiance response models requires initial parameter estimates to initiate the fitting process. Additionally, the selected model must accurately represent the experimental data, as not every model will be suitable for every dataset. Poor model selection and inappropriate starting values can lead to several issues: (1) Increased processing time, as the fitting algorithm takes longer to converge to a solution; (2) Failure to converge, resulting in a higher number of NA pixels; (3) An increased number of incorrect parameter estimates, leading to a higher global RMSE.

To facilitate the selection of appropriate starting values, *pamfit* includes a mandatory step in which users can explore the image by clicking on selected pixels and observing how this choice affects the estimation of P–I curve parameters. These estimations also depend on the model selected by the user. To illustrate the flexibility of *pamfit*, we used the dataset with the highest contrast in photosynthetic parameters — namely, the MPB biofilm, where a drop of dithiothreitol (DTT) was added to the sediment surface. We selected two sets of starting values: one based on a pixel within the DTT-treated region and another from a pixel outside this region (Fig. 2A).

The pixel within the DTT-treated region exhibited significant photoinhibition at the highest light levels, whereas the pixel selected outside this region showed no evidence of photoinhibition (Fig. 2B). The model-fitting algorithm used in *pamfit* demonstrated considerable flexibility, with no differences in RMSE within each model, regardless of the pixel chosen for the initial parameter estimates (Fig. 2C). However, significant differences were observed between models. The highest global RMSE was obtained with the Jassby model (2.82), while the Platt (2.28) and EP (2.28) models showed no significant differences (Fig. 2C).

The Jassby model constrains the PI curve to level off at high irradiances, meaning it cannot accommodate datasets where the response either decreases or continues to increase —both of which were observed in the MPB sample. Specifically, pixels within the DTT-treated region showed a strong decline in rETR at high light levels (Fig. 2B) and often failed to reach saturation at the sample edges. This limitation resulted in higher RMSE values in these regions when using the Jassby model (Fig. 2D). In contrast, the Platt and EP models demonstrated greater flexibility, yielding lower overall RMSE values, particularly in the DTT-affected region (Fig. 2E,F).

Processing time and parallelization

Non-linear iterative processes are computationally intensive operations. The two primary factors influencing execution time were the type of model used and the size of the image being processed (Fig. 3A). Among the models, the Platt model had the longest processing time, whereas the EP model was, on average, 40% faster, and the Jassby model was 60% faster (Fig. 3A, inset). Using a single CPU core, processing a 306,720-pixel image with the Platt model took 9.6 min, whereas the same image was processed in 4.2 min using the EP model (Fig. 3A). The Jassby model was the fastest because it estimates only two parameters (α and ETR_{max}), while the Platt

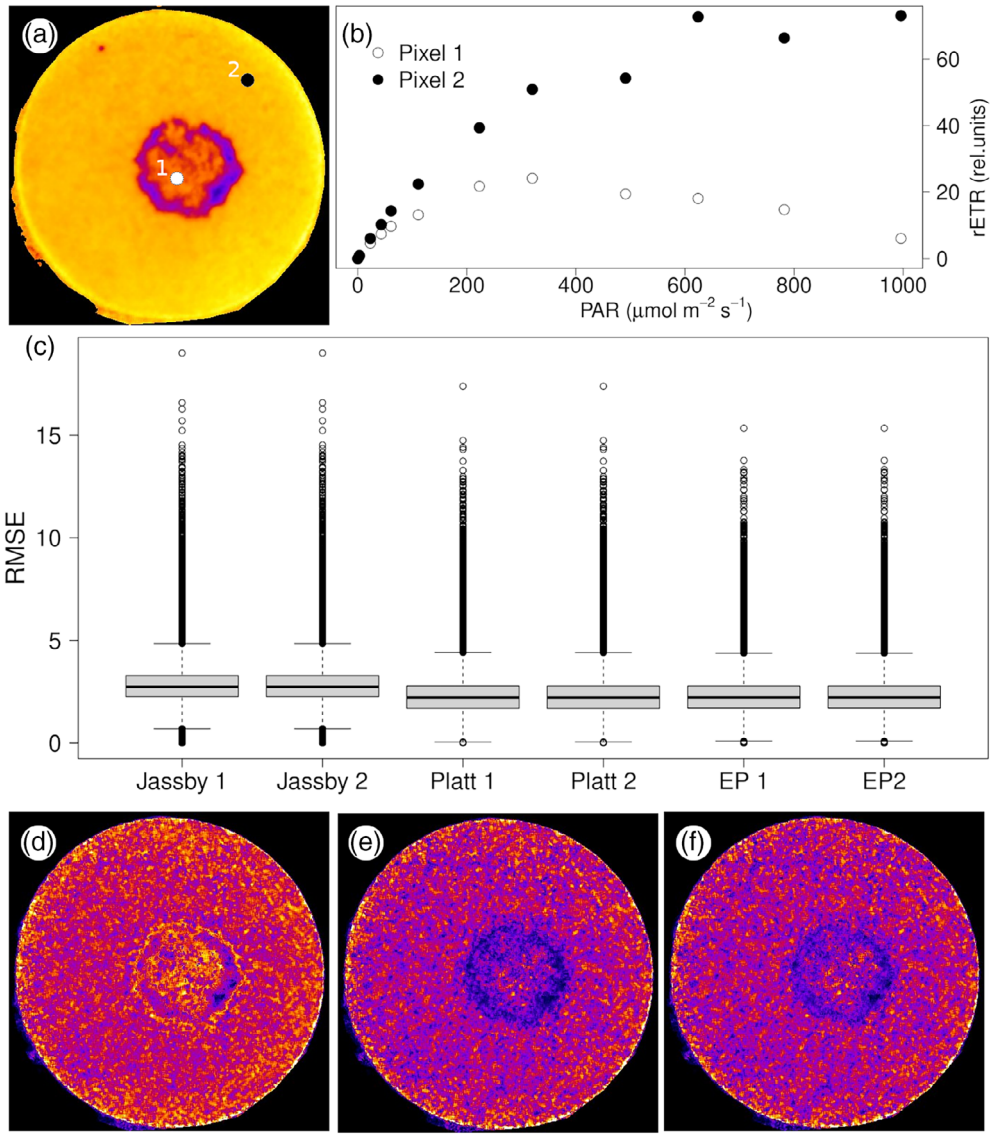

Fig. 2. Effect of parameter starting values and fitting model selection on root mean square error (RMSE). (**a**) Relative electron transport rate (rETR) image of microphytobenthic biofilm at 43 μmol photons m^{-2} s^{-1}, the two numbers represent the two pixels used for the two sets of starting values; (**b**) rETR vs. light plots for the two pixels on panel A; (**c**) RMSE boxplots for each fitting model using the starting values of pixel 1 and pixel 2; RMSE images for the Jassby (**d**), Platt (**e**), and EP (**f**) models.

and EP models estimate three parameters (α, P_s, and β for Platt; α, $\mathrm{ETR_{max}}$, and E_{opt} for EP). The longer computation time for the Platt model is due to the complexity of its parameter calculations. While the Jassby and EP models only compute E_k ($\mathrm{ETR_{max}}/\alpha$), the Platt model calculates $\mathrm{ETR_{max}}$ using a more complex equation involving all three estimated parameters:

$$\mathrm{ETR_{max}} = P_S \times (\alpha/[\alpha+\beta]) \times (\beta/\alpha+\beta)^{(\beta/\alpha)}$$

Modern computers are usually equipped with multiple CPU cores, so we designed our code to support parallel processing, distributing computations across available cores to improve processing speed. To achieve this, we utilized the *raster* package (Hijmans 2023) in R, specifically the *clusterR()* function. Parallel processing significantly reduced execution time (Supporting Information Tables S2–S4), with a clear dependency on image size and a minor effect of the selected model. In general, larger images benefited more from parallelization. The *clusterR()* function divides the raster into chunks and processes them in parallel across multiple cores. However, this splitting process introduces computational overhead, and beyond a certain point, the additional time required for splitting outweighs the gains from parallel processing. Thus, the optimal balance depended on both image size and model type

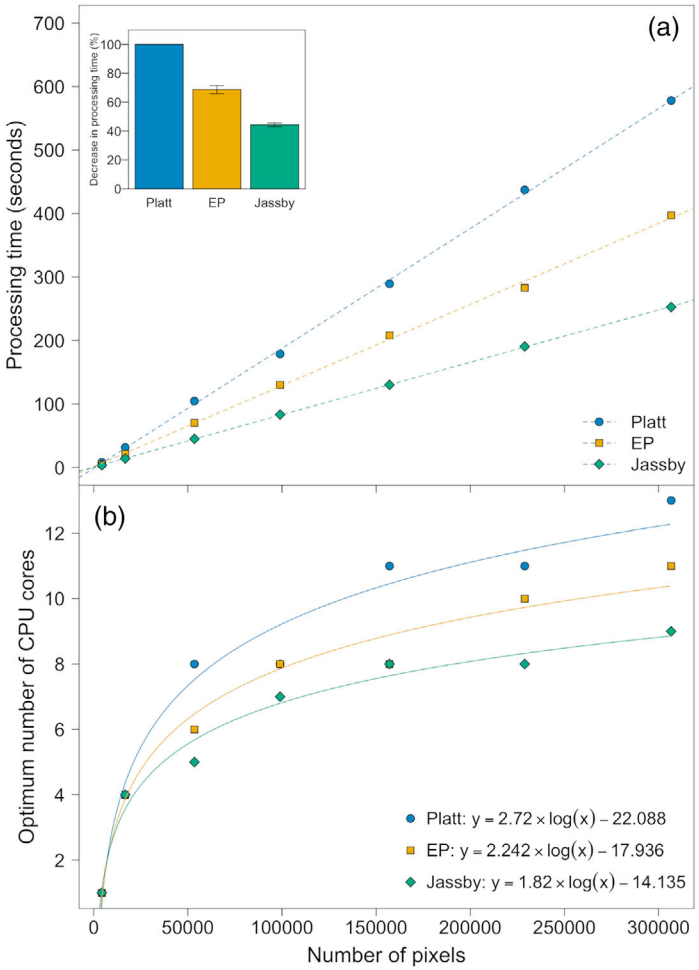

Fig. 3. Central processing unit (CPU) processing time in minutes using a test image of 640 × 480 pixels resized to different sizes, calculations done with an 3rd Gen Intel® Core™ i9-13950HX (32 threads). (**a**) Processing time in seconds of images of increasing size and for the three models; inset in (A) represents the time difference using the slowest model (Platt) as reference; (**b**) optimum number of CPU cores to use depending on the chosen model (Jassby, Platt, and EP) and the size of the image.

(Fig. 3B). The Platt model benefited the most from parallelization, with the largest image processing fastest at 12 cores. In contrast, the same image fitted with the Jassby model showed no further speed improvements beyond 9 CPU cores. Splitting calculations across two cores immediately improved processing speed, except for the smallest image (4305 pixels), which was too small to gain any advantage from parallel processing. In the most computationally intensive scenario, that is, the Platt model applied to the largest image (306,720 pixels), switching from a single core to two cores reduced processing time by 54%.

It is important to note that all tests were conducted on Unix-based systems (Linux and macOS). The *clusterR()* function is less efficient on Windows systems, as it launches multiple R sessions, which may cause memory issues and lead to slower processing (Hijmans 2023). We observed mixed results when testing our code on Windows machines, so we recommend that Windows users first run single-core processing (i.e., the default) before attempting parallelization on their systems.

Real-world applications

Photosynthesis–irradiance (P–I) curve parameters serve as valuable indicators of an organism's photophysiological status. For photosynthetic tissues, these parameters can help distinguish areas where different photophysiological processes are occurring, for example, identifying regions affected by varying degrees of photoinhibition (β), areas with different photosynthetic capacities (ETR_{max}), or zones with higher light-use efficiencies (α).

The following sections provide examples of how P–I curve parameter images can be used, along with some of their limitations. While the examples focus on kleptoplastidic sea slugs, microphytobenthic biofilms, and the red alga *C. officinalis*, these image analysis techniques can be applied to any photosynthetic structure measurable with an Imaging PAM fluorescence system, including corals, other types of macroalgae, and both aquatic and terrestrial plants.

Transect analysis

A common approach to analyzing continuous photosynthetic surfaces is to perform transects to detect changes and patterns (e.g., Perkins et al. 2016). The *pamfit* Shiny app allows users to explore sample surfaces interactively by drawing transects with the mouse. After running *pamfit* and generating P–I curve parameter images, users can conduct transects on any P–I curve parameter image to examine spatial variations in photosynthetic properties. We present three example transect analyses.

The first is a transect of ETR_{max} across the transverse section of *E. timida*'s body, showing how ETR_{max} values increase from the periphery toward the middle of the sea slug's parapodia, then decrease toward the central axis, with this pattern repeating in the other parapodia (Fig. 4A,B). The slug's digestive system is a highly branched structure that extends throughout most of the body but is concentrated in the center of the parapodia (Marín and Ros 1993; Cartaxana et al. 2019). The observed ETR_{max} gradient from the center to the periphery suggests that kleptoplast efficiency is not uniform across the animal's surface. One possible explanation is that kleptoplasts undergo progressive degradation from the main digestive tube to the smaller peripheral branches.

The second example examines an MPB biofilm where DTT was applied to the sediment surface (Fig. 4C). Dithiothreitol is a potent inhibitor of the xanthophyll cycle, the primary photoregulatory mechanism in diatoms (e.g., Lavaud et al. 2004; Jesus et al. 2008; Domingues et al. 2012). A visual

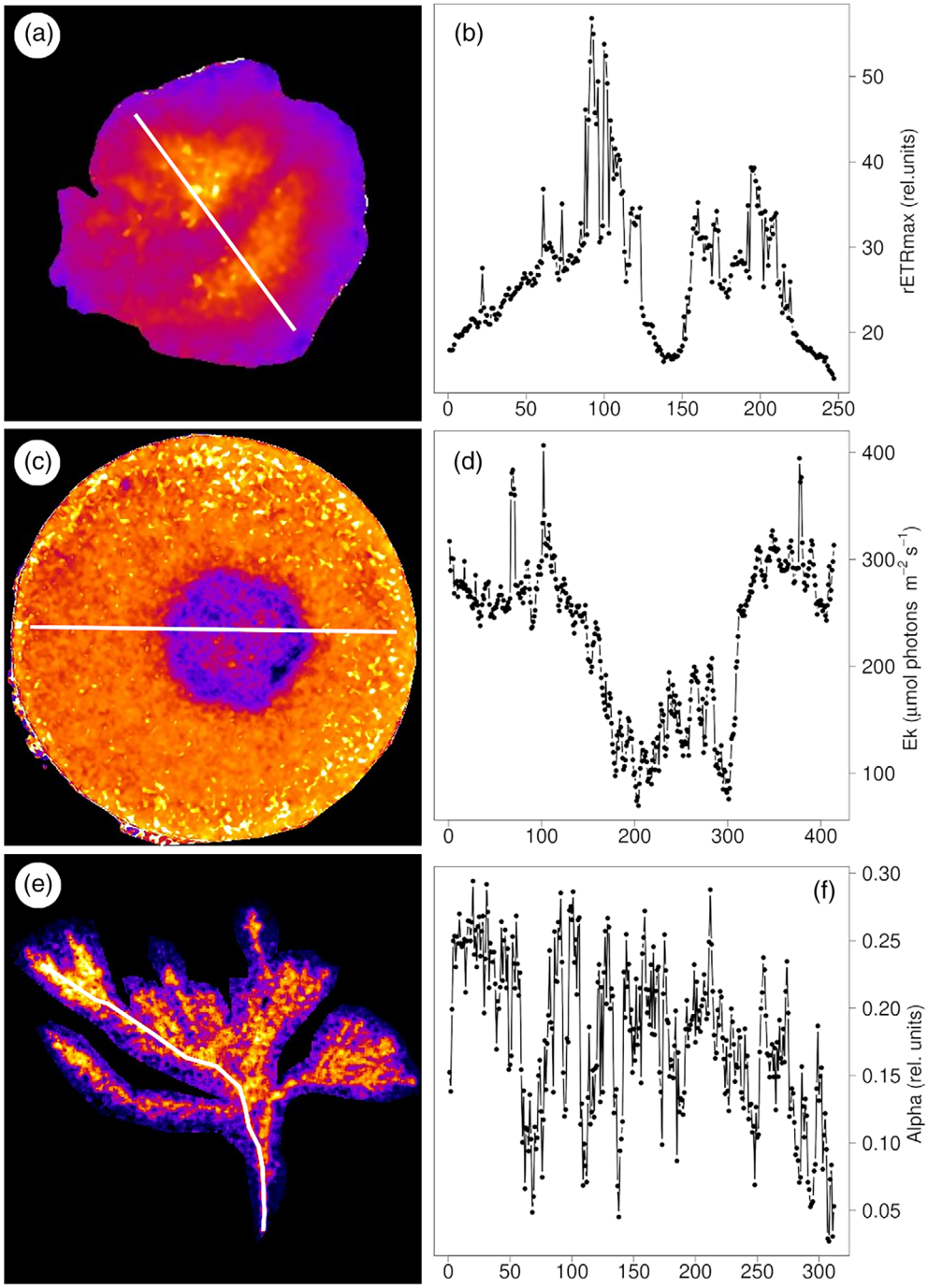

Fig. 4. Examples of a transect analysis on P–I curve parameter images. (**a**) Maximum relative electron transport rate ($_rETR_{max}$) image of *Elysia timida* and an overlaid transect (white line); (**b**) $_rETR_{max}$ values of the pixels covered by the transect. (**c**) Light saturation coefficient (E_k) image of a microphytobenthic biofilm and a transect that intersects a section where the dithiothreitol (DTT) inhibitor (center of the image) was added; (**d**) E_k values of the pixels covered by the transect in panel C; (**e**) Light utilization coefficient (α) image of a *Corallina officinalis* frond and a transect going from the tip to the base of the frond; (**f**) α values of the pixels covered by the transect in panel E.

analysis of the E_k image clearly shows that DTT had a strong effect on this parameter, reducing it to approximately one-third its maximum value in the treated areas (Fig. 4D). Plotting a transect across the surface further highlights the regions affected by DTT, revealing an edge effect at the boundary between the treated and untreated sediment (Fig. 4D), which was likely due to the accumulation of DTT at the periphery of the droplet.

The final example involves mapping the α parameter in a *C. officinalis* frond and analyzing a transect from the tip to the base of the frond (Fig. 4E). The algae in this example were heavily colonized by diatoms at the upper extremities, with decreasing epiphyte coverage toward the base, where the macroalgal tissue was nearly free of epiphytes (*see* Perkins et al. 2016, for details). This resulted in several gradients in photophysiological parameters. Here, we highlight the α parameter, which exhibited a clear decreasing trend from the tip to the base of the frond (Fig. 4F), likely due to variations in epiphyte coverage. The high density of diatom epiphytes at *C. officinalis frond* tips could result in strong light attenuation and self-shading effects, which likely contributed to the higher α values observed (Fig. 4E).

Region of interest analysis

Users often need to compare different sections of an image. *pamfit* facilitates this by allowing the selection of regions of interest (ROI) on any of the generated parameter images (e.g., α, E_k, $\mathrm{ETR_{max}}$) or raw data images (e.g., F_o, F_m, F_v/F_m, etc.). This feature enables a quick and intuitive preliminary visual analysis of different regions. By drawing an ROI with the mouse, users can generate a boxplot comparing two selected parameters. Additionally, all pixels within the selected ROI can be exported to the R workspace or saved as a text file (.csv) for external processing. We demonstrate this functionality with three applications from our datasets.

The first example uses the E_k parameter image of the sea slug (Fig. 5A). By selecting one ROI in the center of a parapodium and another near its edge, we observed significant differences in the E_k parameter between the two regions (Fig. 5B). The lower E_k values at the periphery are likely due to increased degradation of kleptoplasts toward the outer edges of the slug's digestive system.

The MPB transect analysis revealed a sharp decline in E_k at the edge of the DTT-treated region. To further investigate whether this pattern was also reflected in $\mathrm{ETR_{max}}$, we selected three ROI on the $\mathrm{ETR_{max}}$ image: one around the DTT edge, a second within the DTT-treated region, and a third outside the DTT-affected area (Fig. 5C). Boxplot analysis showed clear and significant differences among the three ROI (Fig. 5D), with the highest $\mathrm{ETR_{max}}$ values observed outside the DTT region and the lowest at the DTT edge. This confirms the previous observation that the DTT effect was strongest at the boundary of the treated zone compared to its center.

For the *Corallina* example, an $\mathrm{ETR_{max}}$ image was selected and ROI defined in areas with known differences in epiphyte coverage. Specifically, we placed one ROI at the frond tips, another in the middle section, and a third at the base of the frond (Fig. 5E). Boxplot analysis revealed that the middle section had the highest $\mathrm{ETR_{max}}$ values (Fig. 5F). The other two ROI showed lower $\mathrm{ETR_{max}}$ values, with the lowest observed at the base of the frond, likely due to frequent shading from the rest of the algae.

The ROI analysis section in *pamfit* enables the statistical evaluation of P–I curve parameter images using dispersion measurements, such as medians and quartiles, as demonstrated in our boxplot examples. By incorporating pixel-level variability, this approach allows for statistical comparisons between different ROIs. In contrast, integrating areas before fitting the P–I curve model would yield a single parameter value for each region, eliminating information about underlying spatial variability. *pamfit*'s ROI analysis thus provides a more detailed and robust assessment of differences across photosynthetic surfaces.

XY relationships

One valuable application of P–I curve parameter images is their ability to be overlaid with other images, enabling numerical analyses between corresponding pixels. By overlaying P–I curve parameter images with original F_o, F_m, or PSII quantum efficiency images, relationships between different variables can be investigated. In the example shown in Fig. 6, an F_v/F_m image (Fig. 6A) was plotted against an α image (Fig. 6B), revealing a strong linear relationship between the two parameters (Fig. 6C). Decreases in maximum PSII quantum efficiency (i.e., F_v/F_m) are often observed as a response to environmental stress (Adams and Demmig-Adams 2004). The linear trend apparent here between α and F_v/F_m suggests that the kleploplasts inside the animal are at different degradation stages and that the ones with higher F_v/F_m values are capable of achieving higher electron transport rates at lower light levels.

XY analyses can also be performed using data subsets from ROIs selected by the user based on specific criteria. To illustrate this, we used the MPB biofilm image to analyze the relationship between F_v/F_m (Fig. 6D) and $\mathrm{ETR_{max}}$ (Fig. 6E) across the three regions identified in the boxplot analysis, that is, around the DTT edge, inside the DTT-treated region, and outside the DTT-affected area (Fig. 6E). Each ROI exhibited a distinct linear relationship between F_v/F_m and $\mathrm{ETR_{max}}$ (Fig. 6F). Both the DTT-treated and untreated regions showed significant positive relationships ($p < 0.001$), though with different slopes, intercepts and very high dispersion ($R^2 = 0.12$ and 0.10, respectively). Interestingly, the DTT edge displayed the opposite trend, with $\mathrm{ETR_{max}}$ decreasing as F_v/F_m increased ($R^2 = 033$, $p < 0.001$). This unexpected result highlights how exploratory spatial analyses can generate novel research hypotheses, encouraging further targeted experiments to better understand these patterns.

Derived parameters (NPQ analysis)

The *pamfit* Shiny app is currently designed to generate *rETR* parameter images, but the exported analysis objects contain all standard PAM fluorescence parameter images (e.g., F_o, F_m, F', F_m'). The app's workflow allows for further image processing in R, enabling the exploration of additional derived parameters, such as non-photochemical quenching (NPQ). See

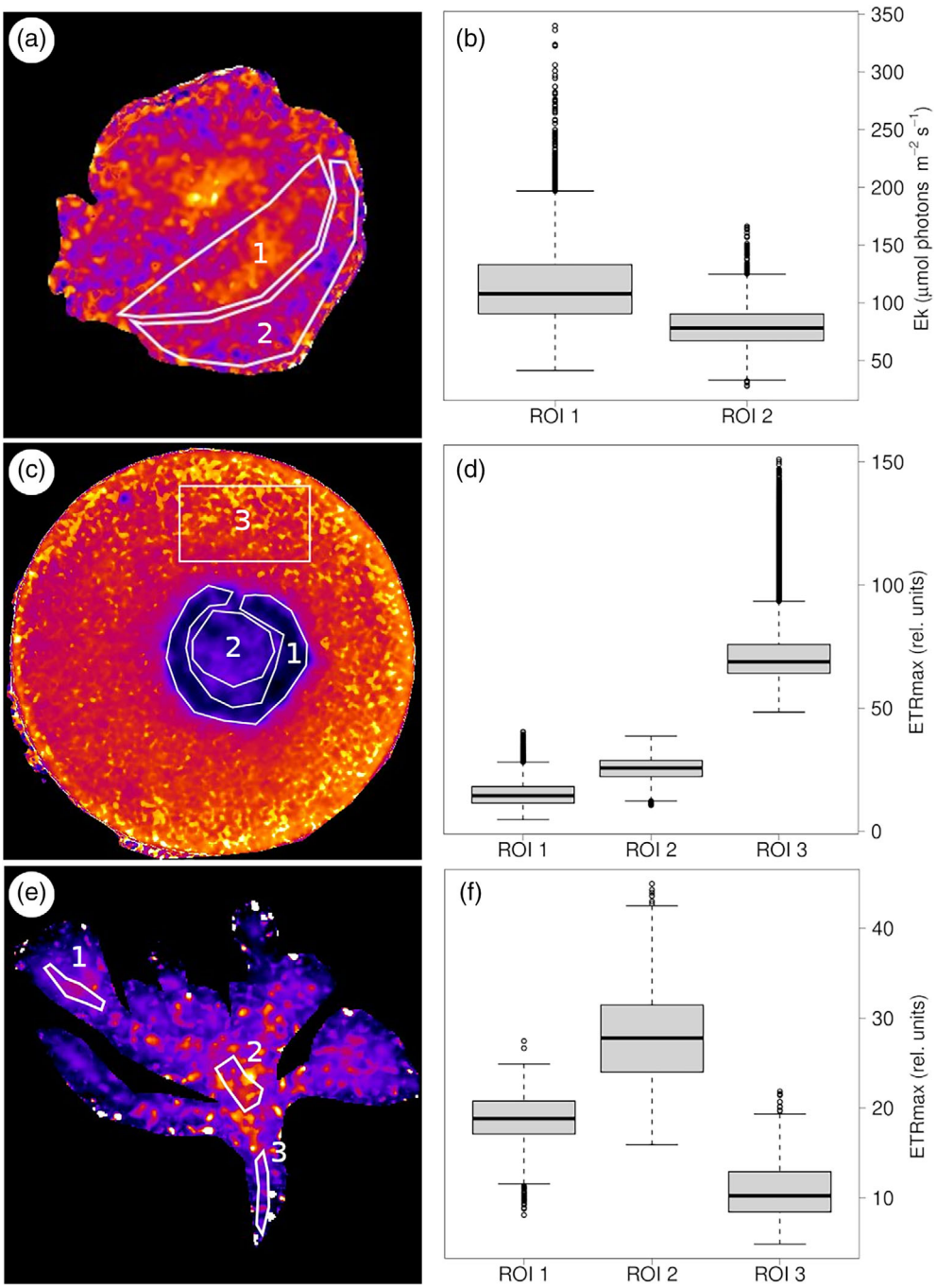

Fig. 5. Examples of regions of interest (ROI) analysis on P–I curve parameter images. (**a**) *Elysia timida* light saturation coefficient (E_k) image and two ROI; (**b**) boxplot results of the ROI in panel A; (**c**) Microphytobenthos maximum relative electron transport rate ($_rETR_{max}$) image and three ROI; (**d**) boxplot results of the ROI in panel D; (**e**) *Corallina officinalis* $_rETR_{max}$ image and three ROI for analysis; (**f**) boxplot results of the ROI in panel E.

the companion document "User guide" (https://github.com/bmjesus/pamfit) for an example of how to calculate NPQ using *pamfit* results.

To illustrate this capability, we analyzed the *Corallina* sample (Fig. 7). First, the sample was processed using the *pamfit* workflow, including pixel smoothing, ROI selection, and *ETR* model fitting. The results were then exported to the R workspace, where NPQ images were calculated for each light step using the equation: $NPQ = (F_m - F_m')/F_m'$. A clear spatial pattern emerged, with *Corallina* frond tips exhibiting much higher NPQ values compared to the central and basal regions (Fig. 7A,I).

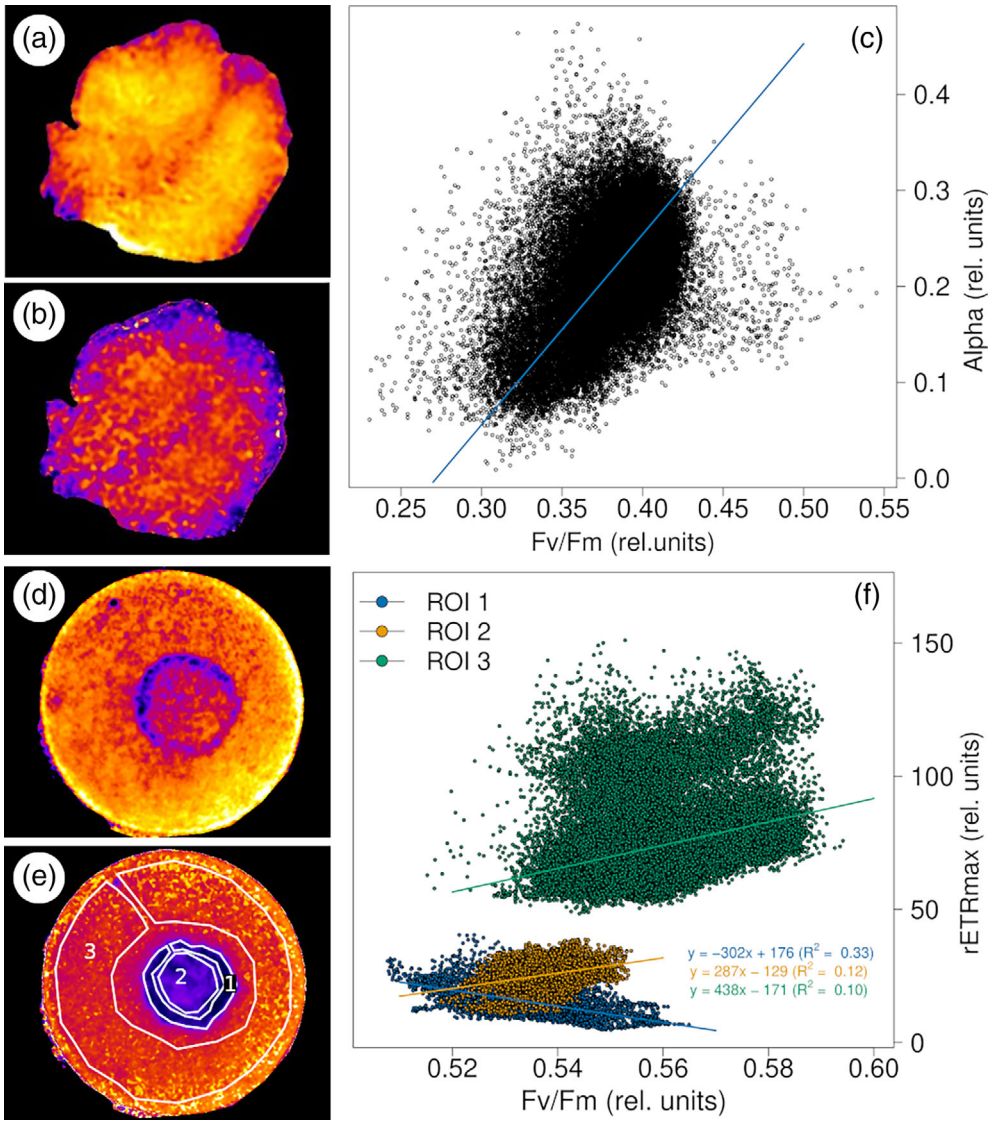

Fig. 6. Examples of X–Y relationships between images or regions of interest (ROI). (**a**,**b**) *Elysia timida* maximum photosynthetic efficiency (F_v/F_m) and light utilization coefficient (α) images, respectively; (**c**) XY scatterplot of F_v/F_m and α pixel values showing the linear relationship between these two variables; (**d**, **e**) F_v/F_m and maximum relative electron transport rate ($_rETR_{max}$) images of a microphytobenthic biofilm, respectively, and three ROI for analysis; (**f**) XY scatterplot of F_v/F_m and $_rETR_{max}$ pixel values showing the linear relationship between these two variables at the three ROI seen on panel E.

In a previous study, Perkins et al. (2016) investigated the rETR patterns of these samples and concluded that most of the observed differences could be attributed to variations in epiphyte coverage. The tips of low-shore *Corallina* samples—like the one analyzed here—were densely colonized by diatoms (*see* Fig. 2 in Perkins et al. 2016). Diatoms are known to exhibit higher NPQ values compared to other algae (Bailleul et al. 2010). To further analyze these patterns, we selected three ROI (Fig. 7I) and plotted NPQ values against light intensity. The results clearly showed that pixels corresponding to diatom-covered regions had significantly higher NPQ levels (Fig. 7J). Fitting these values with the NPQ model described in Serôdio and Lavaud (2023) yielded NPQ_{max} values of 5.4, 3.1, and 1.32 for the tip, middle, and base of the frond, respectively. Currently, pamfit only calculates ETR-derived parameters but future versions will include other fluorescence parameters, for example, NPQ, YNO, and so forth.

Discussion

The *pamfit* R package was developed to fill a methodological gap in Imaging PAM fluorescence data analysis. While proprietary software enables calculation of relative electron transport rates (rETR) for selected regions of interest, it does

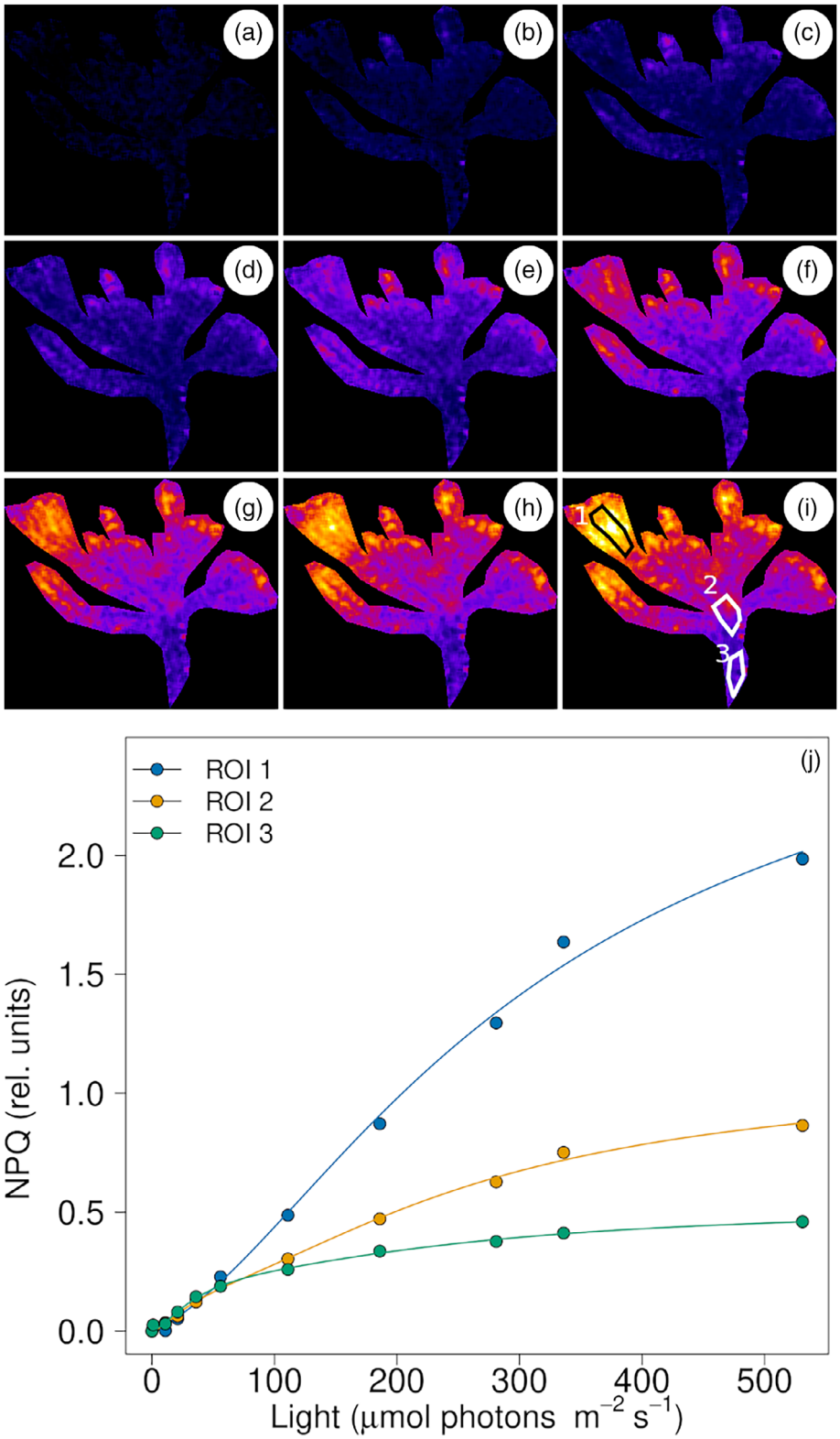

Fig. 7. *Corallina officinalis* non-photochemical quenching (NPQ) images at the P–I curve light steps 11, 21, 36, 56, 111, 186, 281, 336, 531 μmol photons m^{-2} s^{-1} (**a**–**i**); (**j**) NPQ values for the three regions of interest (ROI) drawn on panel I, lines are predicted NPQ values after fitting the model described in Serôdio and Lavaud (2023).

not permit pixel-wise modeling of photosynthesis–irradiance (P–I) curves across an entire image. This limitation stops researchers from fully exploring the spatial variability of photosynthetic surfaces. *pamfit* addresses this limitation by implementing automated pixel-wise model fitting using open-source tools (i.e., R shiny app), thus enabling the generation of complete parameter images (e.g., α, E_k, ETR_{max}, β). *pamfit* does this using an integrated Shiny interface that manages the complete workflow (from image import to parameter modeling and export) while maintaining accessibility for users with limited R programming experience. Its ability to fit non-linear models pixel-by-pixel allows users to retain spatial information and transforms Imaging PAM fluorescence data from region-averaged summaries into spatially explicit datasets suitable for quantitative map-based analyses. This implementation represents a fundamentally new approach. Although the underlying models (e.g., Jassby and Platt 1976; Platt et al. 1980; Eilers and Peeters 1988) are well established in photosynthesis research, their automated, spatially resolved application to Imaging PAM fluorescence datasets has not previously been implemented. The integration of multi-core parallelization, uncertainty estimation, and flexible model choice further distinguishes *pamfit* from existing workflows.

Notably, the possibility of having quantitative maps of photosynthetic parameters enables new types of analyses that were previously impractical. Namely, spatial gradients in α, ETR_{max}, or E_k can now be correlated with structural, physiological, or environmental features, such as chloroplast distribution, tissue organization or surface heterogeneity. The ability to overlay P–I parameter images with other spatial data (e.g., temperature maps, oxygen optode imagery, hyperspectral imagery, or micro-topography) creates the opportunity for multi-dimensional eco-physiological analyses that could not be solved otherwise. In the examples we provided (*E. timida*, microphytobenthic biofilms, *C. officinalis*), *pamfit* revealed fine-scale spatial heterogeneity and patterns consistent with known physiological processes, demonstrating its potential to generate new hypotheses about photoregulation and stress responses. Imaging PAM fluorometry can be applied at a wide range of spatial scales, from sub-cellular organelles to macro-organism scales. Thus, *pamfit* has the potential to enable new insights into photosynthetic variability across multiple-biological scales.

Comments and recommendations

The *pamfit* Shiny app performed well across all tested samples. However, there are some recommendations and potential limitations that users should consider.

Applying a small degree of smoothing consistently improved the results (Fig. 1), likely by reducing electronic noise inherent to the image acquisition process. We recommend that users identify the optimal smoothing level, that is, the "sweet spot," where noise is minimized without significant loss of spatial variability. In our samples, smoothing at three to five pixels consistently enhanced the results without compromising spatial structure.

The selection of model parameter starting values plays a crucial role in the fitting process. The PORT non-linear least-squares fitting algorithm demonstrated strong robustness to high spatial variability (Fig. 2). However, if an image contains extreme differences in P–I curve response patterns, the selected pixel for the initial parameter estimates may significantly influence the results. To ensure consistency, we recommend that—if possible—samples with extreme differences be analyzed separately, using distinct images rather than a single composite image. This approach helps minimize potential biases introduced by variations in starting values.

Using a model that includes a photoinhibition component (i.e., Platt or EP) consistently resulted in lower global RMSE values (Fig. 2). However, this came at the cost of increased processing time, with the Platt model requiring more than twice the time of the Jassby model (Fig. 3). Therefore, if processing time is a limiting factor and the dataset does not exhibit signs of photoinhibition, the Jassby model can be used as a faster alternative. Otherwise, the Platt and EP models generally provide better results.

Parallel processing was highly beneficial for large images, significantly reducing processing time (Supporting Information Tables S2–S4). However, the greatest performance gains were observed between two and four CPU cores. Beyond this, increasing the number of cores resulted in only minor improvements or, in some cases, even slower processing. We provide the observed relationship between optimal CPU core usage and image size as a reference (Fig. 3B), but we recommend that users test processing speed on their own systems to determine the most efficient configuration. Memory limitations may occur when running *pamfit* in parallel mode, particularly on Windows systems where *clusterR()* launches multiple R sessions. Processing several images in a single session without closing pamfit can also increase memory usage, as RStudio retains objects until they are released to the workspace when *pamfit* is closed. The safest approach is to run *pamfit* in serial mode (one CPU core) and process one image per session. However, in most systems we tested, using two cores was stable and halved processing time.

Fitting the P–I curve models may occasionally produce infinite or extreme values. Infinite values are handled internally by pamfit and excluded from calculations and image rendering. However, extreme outliers are retained and can distort the output by stretching the color scale, often resulting in mostly dark images with isolated bright pixels. This is a visual artifact of the outlier presence and can be manually compensated by the user by inputting the minimum and maximum values in the color range input boxes. Finding the pixel values can be easily done by clicking on the image with the mouse.

The functionality of opening processed TIFF files relies on the *metags* function from the *Terra* package, which generates the metadata associated with each data layer. In the current *pamfit* version, the *metags* function used to open processed

files must be the same version that was used to generate them. For more details please see the user guide for *pamfit* (https://github.com/bmjesus/pamfit).

Imaging PAM technology is a powerful tool for detecting spatial features in a wide range of photosynthetic surfaces. Its potential is further enhanced when used interactively with *pamfit* to generate and analyze P–I curve parameter images. The ability to process these images using free, open-source software extends the applicability and accessibility of this technique. Once P–I curve parameter images are created, they can be integrated into spatial analysis workflows, such as GIS software, where they can be analyzed similarly to satellite reflectance images. Additionally, they can be overlaid with vector-based data, such as point measurements (e.g., temperature readings), to explore spatial relationships between environmental variables and photosynthetic responses. The tools presented in this study demonstrate significant potential for further applications in ecophysiological research, providing new opportunities for spatially explicit analyses of photosynthetic processes.

Author Contributions

B. Jesus: Conceptualization (equal), data curation (lead), formal analysis (equal), funding acquisition (equal), methodology (lead), software (equal), visualization (lead), writing—original draft (lead), writing—review and editing (equal). P. Cartaxana: Conceptualization (equal); funding acquisition (equal); methodology (supporting); writing—review and editing (equal). C. Williamson: Conceptualization (supporting); data curation (supporting), formal analysis (equal), funding acquisition (equal), methodology (supporting), software (equal), writing—original draft (supporting), writing—review and editing (equal).

Acknowledgments

This project has received funding from the European Union's Horizon 2020 research and innovation program under the Marie Skłodowska Curie grant agreement No 860125 (BEEP) and by the European Union under Grant Agreement 101081357 (REWRITE). C. Williamson was supported by the Leverhulme Trust "iDAPT" Research Project award (RPG-2020-199) and the National Environmental Research Council "CASP-ICE" award (NE/Y002636/1). P. Cartaxana was funded by Fundação para a Ciência e Tecnologia, grant CEECIND/01434/2018 (https://doi.org/10.54499/CEECIND/01434/2018/CP1559/CT0003). The authors thank Sónia Vieira for helping with the microphytobenthic sampling and with the Imaging PAM measurements.

Conflicts of Interest

None declared.

Data Availability Statement

All code and example datasets are freely available via GitHub at: https://github.com/bmjesus/pamfit.

References

Adams, W., III, and B. Demmig-Adams. 2004. "Chlorophyll Fluorescence as a Tool to Monitor Plant Response to the Environment." In Chlorophyll a Fluorescence: A Signature of Photosynthesis, edited by G. C. Papageorgiou and Govindjee, 583–604. The Netherlands: Springer.

Bailleul, B., A. Rogato, A. de Martino, et al. 2010. "An Atypical Member of the Light-Harvesting Complex Stress-Related Protein Family Modulates Diatom Responses to Light." *Proceedings. National Academy of Sciences. United States of America* 107: 18214–18219. https://doi.org/10.1073/pnas.1007703107.

Cartaxana, P., L. Morelli, B. Jesus, G. Calado, R. Calado, and S. Cruz. 2019. "The Photon Menace: Kleptoplast Protection in the Photosynthetic Sea Slug *Elysia timida*." *Journal of Experimental Biology* 222, no. 12: jeb202580. https://doi.org/10.1242/jeb.202580.

Cartaxana, P., F. Rey, C. LeKieffre, et al. 2021. "Photosynthesis From Stolen Chloroplasts Can Support Sea Slug Reproductive Fitness." *Proceedings of the Royal Society B* 288: 20211779. https://doi.org/10.1098/rspb.2021.1779.

Cheng, J., J. Allaire, C. Sievert, et al. 2024. "*shiny: Web Application Framework for R*." R Package Version 1.8.1.9001. https://github.com/rstudio/shiny; https://shiny.posit.co/.

Costa, J., F. Giménez-Casalduero, R. Melo, and B. Jesus. 2012. "Colour Morphotypes of *Elysia timida* (Sacoglossa, Gastropoda) Are Determined by Light Acclimation in Food Algae." *Aquatic Biology* 17: 81–89. https://doi.org/10.3354/ab00446.

Domingues, N., A. R. Matos, J. Marques da Silva, and P. Cartaxana. 2012. "Response of the Diatom *Phaeodactylum tricornutum* to Photooxidative Stress Resulting From High Light Exposure." *PLoS One* 7, no. 6: e38162. https://doi.org/10.1371/journal.pone.0038162.

Eilers, P. H. C., and J. C. H. Peeters. 1988. "A Model for the Relationship Between Light Intensity and the Rate of Photosynthesis in Phytoplankton." *Ecological Modelling* 42: 199–215. https://doi.org/10.1016/0304-3800(88)90057-9.

Elzhov, T. V., K. M. Mullen, A. Spiess, and B. Bolker. 2023. "*minpack.lm: R Interface to the Levenberg-Marquardt Nonlinear Least-Squares Algorithm Found in MINPACK, Plus Support for Bounds*." R Package Version 1.2-4. https://CRAN.R-project.org/package=minpack.lm.

Gerbersdorf, S., J. Meyercordt, and L.-A. Meyer-Reil. 2005. "Microphytobenthic Primary Production in the Bodden Estuaries, Southern Baltic Sea, at Two Study Sites Differing in Trophic Status." *Aquatic Microbial Ecology* 41: 181–198. https://doi.org/10.3354/ame041181.

Guarini, J.-M., J. Cloern, J. Edmund, and P. Gros. 2002. "Microphytobenthic Potential Productivity Estimated in Three Tidal Embayments of the San Francisco Bay: A Comparative Study." *Estuaries* 25, no. 3: 409–417. https://doi.org/10.1007/BF02695983.

Hijmans, R. 2023. "*raster: Geographic Data Analysis and Modeling*." R Package Version 3.6-26. https://CRAN.R-project.org/package=raster.

Jassby, A. D., and T. Platt. 1976. "Mathematical Formulation of the Relationship Between Photosynthesis and Light for

Phytoplankton." *Limnology and Oceanography* 21: 540–547. https://doi.org/10.4319/lo.1976.21.4.0540.

Jesus, B., T. Jauffrais, E. C. L. Trampe, et al. 2022. "Kleptoplast Distribution, Photosynthetic Efficiency and Sequestration Mechanisms in Intertidal Benthic Foraminifera." *ISME Journal* 16: 822–832. https://doi.org/10.1038/s41396-021-01128-0.

Jesus, B., T. Jauffrais, E. C. L. Trampe, et al. 2023. "Microscale Imaging Sheds Light on Species-Specific Strategies for Photo-Regulation and Photo-Acclimation of Microphytobenthic Diatoms." *Environmental Microbiology* 25, no. 12: 3087–3103. https://doi.org/10.1111/1462-2920.16499.

Jesus, B., M. Marani, V. Brotas, and D. M. Paterson. 2005. "Spatial Dynamic of Microphytobenthos Determined by PAM Fluorescence." *Estuarine, Coastal and Shelf Science* 65: 30–42. https://doi.org/10.1016/j.ecss.2005.05.005.

Jesus, B., J.-L. Mouget, and R. Perkins. 2008. "Detection of Diatom Xanthophyll Cycle Using Spectral Reflectance." *Journal of Phycology* 44, no. 5: 1349–1359. https://doi.org/10.1111/j.1529-8817.2008.00583.x.

Jesus, B., P. Ventura, and G. Calado. 2010. "Behaviour and a Functional Xanthophyll Cycle Enhance Photo-Regulation Mechanisms in the Solar-Powered Sea Slug *Elysia timida* (Risso, 1818)." *Journal of Experimental Marine Biology and Ecology* 395: 98–105. https://doi.org/10.1016/j.jembe.2010.08.021.

Lavaud, J., B. Rousseau, and A. L. Etienne. 2004. "General Features of Photoprotection by Energy Dissipation in Planktonic Diatoms (Bacillariophyceae)." *Journal of Phycology* 40: 130–137. https://doi.org/10.1046/j.1529-8817.2004.03026.x.

Leal, M. C., B. Jesus, J. Ezequiel, et al. 2014. "Concurrent Imaging of Chlorophyll Fluorescence, Chlorophyll *a* Content and GFP-Like Proteins of Symbiotic Cnidarians." *Marine Ecology* 36: 572–584. https://doi.org/10.1111/maec.12164.

Lichtenberg, M., E. C. L. Trampe, T. C. Vogelmann, and M. Kühl. 2017. "Light Sheet Microscopy Imaging of Light Absorption and Photosynthesis Distribution in Plant Tissue." *Plant Physiology* 175: 721–733. https://doi.org/10.1104/pp.17.00820.

Marín, A., and J. Ros. 1993. "Ultrastructural and Ecological Aspects of the Development of Chloroplast Retention in the Sacoglossan Gastropod *Elysia timida*." *Journal of Molluscan Studies* 59: 95–104. https://doi.org/10.1093/mollus/59.1.95.

Morelle, J., A. Bastos, S. Frankenbach, et al. 2024. "The Photoprotective Behavior of a Motile Benthic Diatom as Elucidated From the Interplay Between Cell Motility and Physiological Responses to a Light Microgradient Using a Novel Experimental Setup." *Microbial Ecology* 87: 40. https://doi.org/10.1007/s00248-024-02354-7.

Nielsen, H. D., and S. L. Nielsen. 2008. "Evaluation of Imaging and Conventional PAM as a Measure of Photosynthesis in Thin- and Thick-Leaved Marine Macroalgae." *Aquatic Biology* 3: 121–131. https://doi.org/10.3354/ab00069.

Omasa, K., K. L. Shimazaki, I. Aiga, W. Larcher, and M. Onoe. 1987. "Image Analysis of Chlorophyll Fluorescence Transients for Diagnosing the Photosynthetic System of Attached Leaves." *Plant Physiology* 84: 748–752. https://doi.org/10.1104/pp.84.3.748.

Oxborough, K., A. R. M. Hanlon, G. J. C. Underwood, and N. R. Baker. 2000. "*In Vivo* Estimation of the Photosystem II Photochemical Efficiency of Individual Microphytobenthic Cells Using High-Resolution Imaging of Chlorophyll *a* Fluorescence." *Limnology and Oceanography* 45: 1420–1425. https://doi.org/10.4319/lo.2000.45.6.1420.

Perkins, R. G., C. J. Williamson, J. Brodie, et al. 2016. "Microspatial Variability in Community Structure and Photophysiology of Calcified Macroalgal Microbiomes Revealed by Coupling of Hyperspectral and High-Resolution Fluorescence Imaging." *Scientific Reports* 6: 22343. https://doi.org/10.1038/srep22343.

Platt, T., C. L. Gallegos, and W. G. Harrison. 1980. "Photo-Inhibition of Photosynthesis in Natural Assemblages of Marine Phytoplankton." *Journal of Marine Research* 38: 687–701. https://elischolar.library.yale.edu/journal_of_marine_research/1525.

R Core Team. 2025. R: A Language and Environment for Statistical Computing. Vienna, Austria: R Foundation for Statistical Computing. https://www.R-project.org/.

Ralph, P. J., U. Schreiber, R. Gademann, M. Kühl, and A. W. D. Larkum. 2005. "Coral Photobiology Studied With a New Imaging Pulse Amplitude Modulated Fluorometer." *Journal of Phycology* 41: 335–342. https://doi.org/10.1111/j.1529-8817.2005.04034.x.

Serôdio, J., J. Ezequiel, J. Frommlet, M. Laviale, and J. Lavaud. 2013. "A Method for the Rapid Generation of Non-sequential Light-Response Curves of Chlorophyll Fluorescence." *Plant Physiology* 163: 1089–1102. https://doi.org/10.1104/pp.113.225243.

Serôdio, J., and J. Lavaud. 2023. "A Generalized Model for the Light Response of the Nonphotochemical Quenching of Chlorophyll Fluorescence of Diatoms." In The Mathematical Biology of Diatoms, edited by J. L. Pappas. Scrivener Publishing LLC. https://doi.org/10.1002/9781119751939.ch13.

Vieira, S., L. Ribeiro, B. Jesus, P. Cartaxana, and J. da Marques Silva. 2013. "Photosynthesis Assessment in Microphytobenthos With Conventional and Imaging Pulse Amplitude Modulation Fluorometry." *Photochemistry and Photobiology* 89: 97–102. https://doi.org/10.1111/j.1751-1097.2012.01224.x.

Wickham, H., J. Hester, W. Chang, and J. Bryan. 2022. "*devtools: Tools to Make Developing R Packages Easier*." R Package Version 2.4.5. https://CRAN.R-project.org/package=devtools.

Supporting Information

Additional Supporting Information may be found in the online version of this article.

Submitted 04 September 2025
Revised 29 October 2025
Accepted 02 November 2025